

Vibrational effects in the linear conductance of carbon nanotubes

M. GHEORGHE¹, R. GUTIÉRREZ¹, N. RANJAN², A. PECCIA³, A. DI CARLO³ and G. CUNIBERTI¹

¹ *Institute for Theoretical Physics, University of Regensburg, D-93040 Regensburg, Germany*

² *Institute for Physical Chemistry, Technical University of Dresden, D-01069 Dresden, Germany*

³ *INFM and Dept. of Electrical Engineering, University of Rome “Tor Vergata”, I-00133 Rome, Italy*

PACS. 73.63.-b – Electronic transport in nanoscale materials and structures.

PACS. 73.63.Fg – Nanotubes.

PACS. 63.22.+m – Phonons or vibrational states in low-dimensional structures and nanoscale materials.

Abstract. – We study the influence of structural lattice fluctuations on the elastic electron transport in single-wall carbon nanotubes within a density-functional-based scheme. In the linear response regime, the linear conductance is calculated via configurational averages over the distorted lattice. Results obtained from a frozen-phonon approach as well as from molecular dynamics simulations are compared. We further suggest that the effect of structural fluctuations can be qualitatively captured by the Anderson model with bond disorder. The influence of individual vibrational modes on the electronic transport is discussed as well as the role of zero-point fluctuations.

Introduction. – Carbon nanotubes (CNTs) have become a paradigm in the physics of low-dimensional systems due to their fascinating properties [1]. Especially, the close interconnection between their chirality and their electronic structure make them an ideal candidate for applications in the field of molecular electronics. As a consequence, extensive experimental and theoretical research has been carried out in the past years to clarify their structural and conducting properties [1].

Concerning quantum transport in CNTs, it is theoretically well-established that the linear conductance is quantized in units of $G_0 = e^2/h$ [1]. In the case of metallic tubes, effective low-energy theories as well as tight-binding and *ab initio* calculations have demonstrated that two massless electronic bands with linear dispersion cross the Fermi points at $\mathbf{K}(\mathbf{K}') = +(-)2\pi/3a_0$, a_0 being the CNT lattice constant [1, 2]. As a result, two transport channels per spin are open at the Fermi level E_F , leading to a conductance of $4 \times G_0$. This value is conserved even in the presence of disorder as far as the range of the impurity potential is larger than the nanotube lattice constant [3]. The same is expected to hold in the presence of vibrations

at low but nonzero temperatures, where only long wavelength modes can be excited [4]. This is however not transferable to high temperatures, where additional modes may be activated, or to higher-lying bands, where mixing can lead to additional backscattering.

So far, the interaction of electrons with phonon modes in CNTs has been mainly addressed in periodic systems [5]. It is rather difficult to clarify the interplay between charge transport and coupling to vibrational degrees of freedom in its full generality. This requires a reliable electronic structure method, the calculation of electron-phonon matrix elements and the combination with a transport formalism. Some developments in this direction have recently been presented [6], though the calculations were limited to small molecular systems. In nanotubes, however, the large number of vibrational modes make these approaches computationally very demanding.

Here, we investigate the influence of structural fluctuations on the *elastic* electron transport in single-wall CNTs. We apply a recently proposed computational scheme [7] to shed some light on the influence of vibrational modes on charge propagation in CNTs. The method combines Green function techniques with a density-functional-based (DF) methodology for the electronic properties of the system. Electron-phonon matrix elements are not directly calculated; the effect of the lattice distortions on charge propagation is considered via suitable configurational averaging procedures.

Anticipating our main results, we find that the global effect of thermal fluctuations turns out to be stronger for massive bands than for massless bands, *i.e.* the transmission around the Fermi energy is not appreciably affected by them on the length scales investigated here. Further, we show that the effect of the atomic vibrations on the electron transport can be qualitatively captured by static disorder in the spirit of the Anderson model [8].

System and Methodology. – The system consists of an infinite metallic (4,4) CNT, where a finite section is allowed to vibrate and thus define the *scattering region*, see Fig. 1. The remaining semiinfinite segments of the nanotube constitute the electrodes. This configuration approximately mimics the experimental situation of clamped CNTs [9]. An advantage of this geometry is the possibility of comparing the conductance in presence of thermal fluctuations with the limiting case of a perfect infinite tube, where conductance quantization is obtained. Calculations for semiconducting tubes were also performed [10] and showed that the gap region is not appreciably affected by vibrations, while outside the gap a behavior quite similar to that presented here is obtained. Because of the large number of atoms required to simulate the electrodes, the interface and the vibrating region (scattering region), only short sections of the nanotube were included in the latter (three unit cells). Numerical tests with up to six unit cells have not shown any new qualitative effects when comparing with the present calculations. With increasing number of cells the phonon spectrum will develop features of the infinite system, *e.g.* emergence of precursors of low-frequency acoustic and optical modes. Obviously, our approach can not well describe these long-wave length modes; the main effects we find here are however related to vibrations with energies larger than $80 - 100$ meV ($\sim 640 - 800$ cm $^{-1}$).

The equilibrium geometry at zero temperature was found by conjugate gradient relaxation techniques with a DF-parametrized tight-binding Hamiltonian [11]. For a carbon-based system, we use a minimal $2s2p^3$ valence basis set to expand the electronic eigenstates. All energies are measured henceforth with respect to the Fermi level.

The vibrational degrees of freedom of the scattering region are described within the harmonic approximation. We expect the vibrational modes of CNTs to be well-represented by harmonic potentials, in contrast to previously studied organic molecules [7], where low-frequency anharmonic modes were present (torsional modes).

Our approach accounts for the influence of structural fluctuations on the charge transport

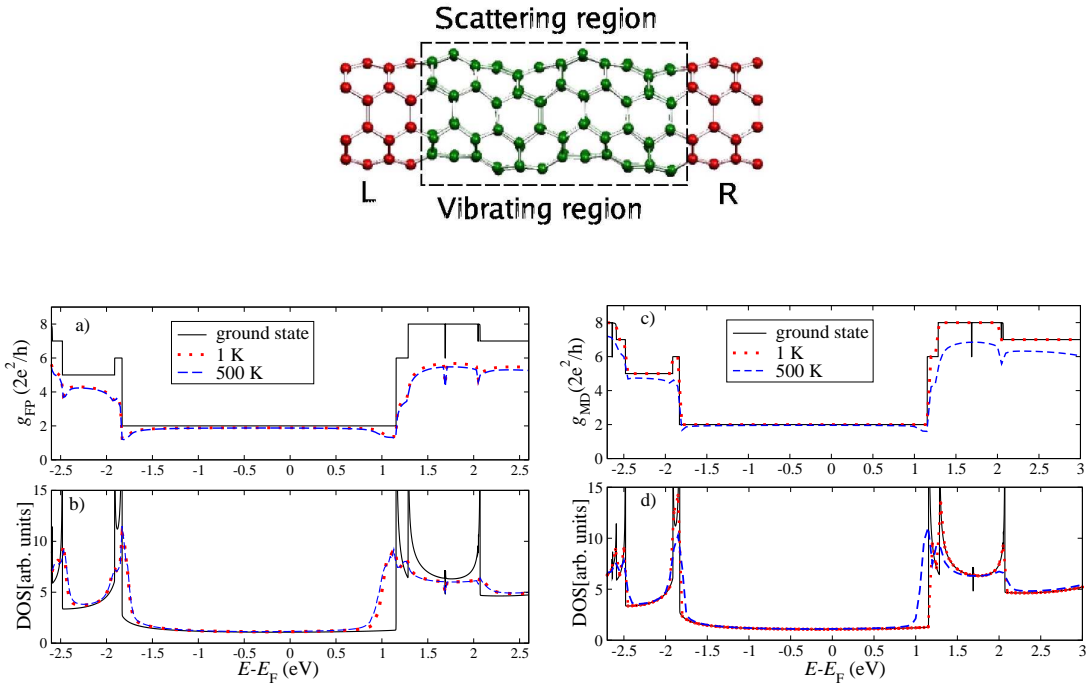


Fig. 1 – Top: snapshot of the vibrating part (scattering region (green)) of an infinite metallic (4x4) CNT. The semiinfinite left (L) and right (R) segments act as electrodes. Bottom: temperature dependence of the conductance spectrum for a (4,4) CNT (a) and corresponding DOS (b), in the frozen-phonon approach. Panels (c) and (d) display the results from molecular dynamics simulations for the same geometry. “Ground state” refers to the zero temperature configuration.

by averaging over sets of atomic configurations $\{\delta\mathbf{r}_\ell\}, \ell = 1, \dots, N$, where N is the number of atoms in the scattering region. We can thus define a configurational averaged *elastic* linear conductance $g(E) = 2G_0 \langle T(E, \delta\mathbf{r}_\ell) \rangle$ [7]. Given an atomic configuration $\{\delta\mathbf{r}_\ell\}$, the transmission can be calculated as $T(E, \delta\mathbf{r}_\ell) = \text{Tr} \{G^\dagger(\delta\mathbf{r}_\ell) \Gamma_R G(\delta\mathbf{r}_\ell) \Gamma_L\}$ [12]. The Green function of the scattering region is given by $G^{-1}(E, \delta\mathbf{r}_\ell) = E S(\delta\mathbf{r}_\ell) - H(\delta\mathbf{r}_\ell) - \Sigma_L - \Sigma_R$. H and S are the Hamiltonian and overlap matrices of the vibrating region with configuration $\{\delta\mathbf{r}_\ell\}$. The overlap matrix takes into account the non-orthogonality of the used basis set. Notice that the influence of the leads has been transferred now into complex self-energy functions $\Sigma_{L,R}$. Finally, $\Gamma_{L,R} = i(\Sigma_{L,R} - \Sigma_{L,R}^\dagger)$ are the corresponding spectral densities of the leads [12].

The linear conductance is calculated within two complementary schemes based on a quantum mechanical resp. classical treatment of the vibrational modes [7]: (i) a frozen-phonon approach (FPA) and (ii) and DF-based molecular dynamics (MD) simulations. Specifically, in the FPA the scattering region is statically distorted according to the eigenvectors of the phonon modes obtained by diagonalizing the dynamical matrix, i. e. via the expansion $\delta\mathbf{r}_\ell = \sum_{\alpha=1}^{3N} x_\alpha \mathbf{e}_\ell^\alpha$ with \mathbf{e}_ℓ^α being the mode eigenvectors. The x_α characterize the amplitude of the atomic displacements, distributed according to $P(\{x_\alpha\}) = \prod_\alpha (\sigma/\sqrt{\pi}) \exp(-\sigma^2 x_\alpha^2)$, with $\sigma^2 = m_\alpha \omega_\alpha^2 / 2E_\alpha(T)$ and $E_\alpha(T) = \hbar\omega_\alpha(N_\alpha(T) + 1/2)$ being the energy of a normal mode [7]. Note that the temperature dependence enters via the Bose factors $N_\alpha(T)$. Using a Monte-Carlo sampling technique, an average conductance $g_{\text{FP}}(E)$ is calculated. In the

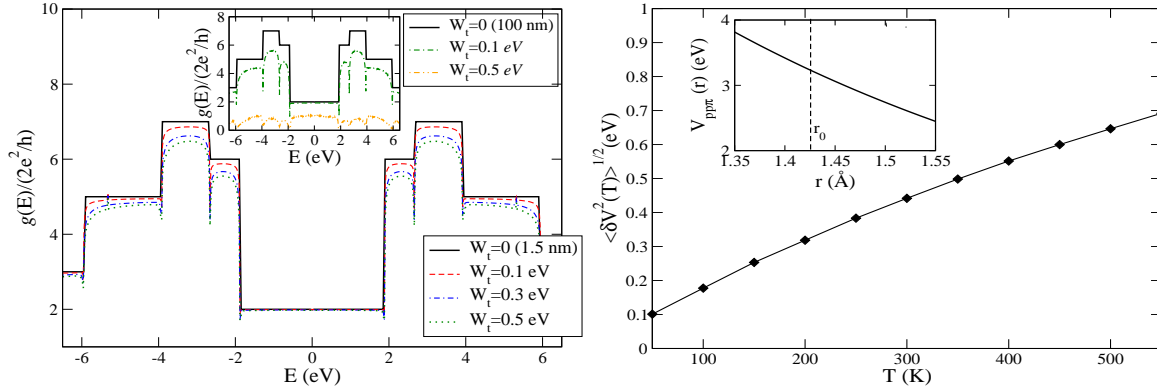


Fig. 2 – Left panel: average conductance obtained from the Anderson Hamiltonian with bond disorder for a short (4 nm) (4x4) CNT. The inset shows similar results for a much longer CNT (100 nm). Right panel: temperature dependence of the average mean-square fluctuation $\sqrt{\langle V^2 \rangle(T)}$ of the $\pi - \pi$ hopping integral. The inset shows the corresponding distance dependence of this matrix element.

MD approach, averages are taken over the simulation time leading to a $g_{\text{MD}}(E)$. Both approaches assume the adiabatic approximation to hold. An estimation of time scale ratios yields $\tau_{\text{phon}}/\tau_{\text{el}}(E_F) \sim 30 - 60$ for phonon energies ≥ 60 meV. Very low-frequency modes may become problematic, but they are not well described when using short CNT sections, as previously mentioned.

Results. – Fig. 1 shows the average conductance as a function of the energy of the incoming electron, calculated for the FP and MD schemes. Both methods yield qualitative similar results. For a CNT at zero temperature and without inclusion of atomic fluctuations, perfect conductance quantization is found, as evident from Figs. 1(a) and 1(c) (solid lines). The corresponding DOS displays the typical van-Hove singularities, see Figs. 1(b) and 1(d) (solid lines).

When taking into account atomic motion, the perfect conductance quantization is washed out, however. Several features can be seen in Fig. 1. The temperature dependence of $g_{\text{FP}}(E)$ is almost negligible on the lowest conductance plateau around the Fermi energy, indicating that backward scattering is considerably weakened in the low-energy sector of the spectrum. Higher-lying bands are however more affected, the conductance being drastically reduced already at 1 K, see Fig. 1(a). Note, however, that upon this initial suppression these bands are not very sensitive to further temperature variations. The reason is that the main contribution to the conductance arises from modes with energies larger than 100 meV ($\sim 1000K$), whose thermal occupation factors are much less than one for the temperature range discussed here (see below). At the crossover points, where new bands start contributing to transport, *e.g.* at energies -2.48 eV, -1.18 eV, and 1.15 eV, conductance dips are found. The corresponding DOS, Fig. 1(b), shows strong broadening of the van-Hove singularities, implying a shift of the spectral weight to their neighboring region. The increased number of states around the crossover points enlarges the phase space for backscattering resulting into the previously mentioned conductance dips.

Let us now consider the results from MD simulations, see Fig. 1(c) and (d). Though the basic features found in the FPA are also seen here, there is however a less abrupt suppression of the conductance of the massive bands with increasing temperature. Thus, at $T = 1 K$

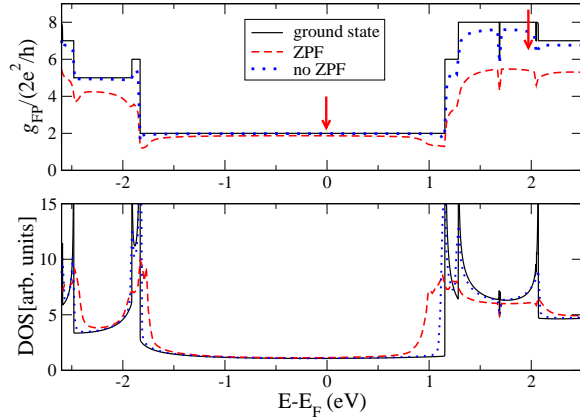


Fig. 3 – The influence of zero-point fluctuations on the conductance of the metallic (4,4) nanotube at a fixed temperature (500 K). Note the strong broadening of the Van-Hove singularities which causes strong conductance dips.

basically no differences to the zero-temperature case can be seen. Even at 500 K, g_{MD} is much closer to the zero temperature case, in contrast to the FPA. This is related to the zero-point fluctuations (ZPF), which are included in the quantum mechanical FP calculation, but are absent in the classical MD approach. The zero-point energy ($\sim \hbar\omega/2$) is inversely proportional to the square root of the atomic mass, so that we may expect that the impact of ZPF on the conductance for a light atom like carbon will be rather strong. Nonetheless, the similarity of the results for the FP and MD approaches indicates that the harmonic approximation is reliable when dealing with the vibrational spectrum of CNTs.

In our calculations, an electron propagating along the vibrating part of the tube will basically feel a quasi-random field. We might expect that some relation to well-known models for disorder may exist. To test this, we have performed calculations based on the Anderson model within a simple π -orbital approximation [8]. The Anderson Hamiltonian reads : $H = \sum_j \epsilon_j c_j^\dagger c_j - \sum_{j,l} t_{lj} [c_j^\dagger c_l + \text{H. c.}]$, where the operators $c_j^\dagger (c_j)$ destroy (create) an electron on the π -orbital at site j . Considering only the π -orbital subspace yields reliable results for CNTs with not too small radii, where $\sigma - \pi$ hybridization can be neglected. Though both, onsite and bond disorder may be considered, we only present results for the latter case. Bond disorder is expected to better mimics the physical situation we are considering here, *i.e.* atomic vibrations, which should mainly influence the C-C bond lengths. Onsite disorder gives qualitative similar results; we thus set $\epsilon_j = 0$ in what follows. The hopping integrals were randomly drawn from the interval $[-W_t + t_{\text{hop}}, W_t + t_{\text{hop}}]$, where $t_{\text{hop}} \sim 2.66$ eV is a typical hopping integral for carbon.

We have performed calculations for short (4 nm) and long (100 nm) nanotubes, see Fig. 2, left panel. One clearly sees that the two basic signatures of structural fluctuations previously found, namely (i) conductance dips at the band crossover points and (ii) conductance suppression on the massive bands, are qualitatively reproduced within the Anderson model. The influence of disorder on the conductance is, as expected, dependent on the CNT length. This is clearly seen at the charge neutrality point, where $g(E_F)$ is much stronger suppressed for longer tubes. From these results, we may expect a relation between W_t and the strength of thermal fluctuations, gauged by $k_B T$. This will lead to a T -dependent disorder parameter $W_t(T)$. However, the differences in the basis sets used in the FPA/MD approaches

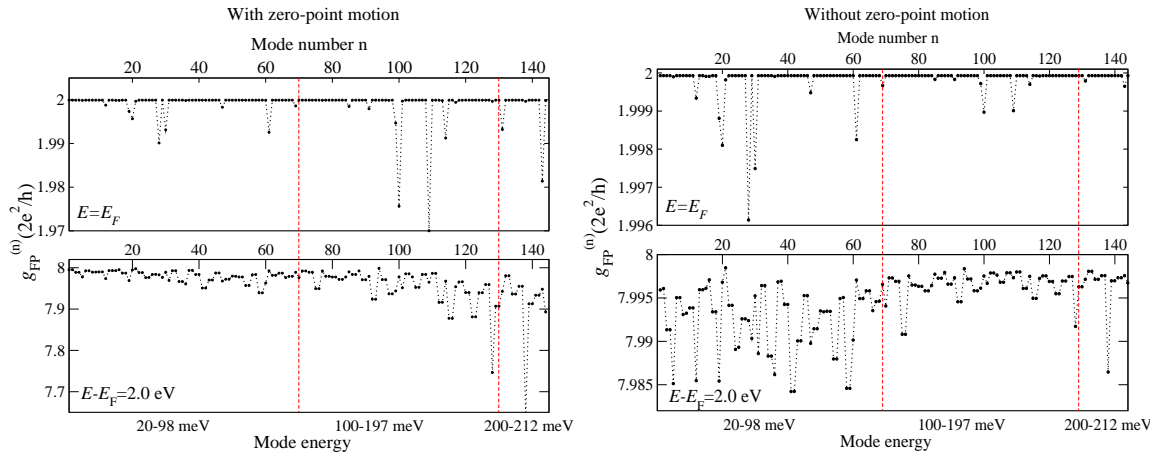


Fig. 4 – Single mode analysis of the conductance at two selected electronic energies, indicated by arrows in Fig. 3, at $T = 500\text{ K}$. The horizontal axis labels the mode number n as well as its energy. Each point in the plot corresponds to the linear conductance $g_{\text{FP}}(E)$ at a given energy E of the incoming electron when just the mode number n is included in the calculation and all other modes excluded. We additionally compare cases with and without inclusion of zero-point fluctuations.

(non-orthogonal $2s2p^3$ basis) and in the Anderson model (π orbitals), respectively, makes a straightforward mapping very difficult. We may get some insight by estimating the temperature dependence of the $V_{pp\pi}$ matrix elements in our DF-based method [11]. The $V_{pp\pi}$ integrals basically describe the interaction of the p_z orbitals and can be thus related to the empirical π -orbital models. We expand them to linear order in the atomic displacements around the equilibrium C–C bond, $r_{\text{CNT}}^0 \sim 1.43\text{ \AA}$, for each atom ℓ in the scattering region: $\delta V_\ell = V_{pp\pi}(\mathbf{r}_\ell) - V_{pp\pi}(r_0) \approx (dV_{pp\pi}/dr)_0 \delta \mathbf{r}_\ell$. From the Monte-Carlo sampling outlined above [7], it is possible to compute an average mean-square fluctuation of the atomic distortions $\langle \delta \mathbf{r}^2 \rangle(T) = \sum_{\ell=1}^N \langle \delta \mathbf{r}_\ell^2 \rangle(T)$, where $\langle \dots \rangle$ is an average over the $P(\{x_\alpha\})$ distribution (see above) and a further average over all atoms in the scattering region has been carried out. The related T-dependent fluctuations $\sqrt{\langle \delta V^2 \rangle(T)}$, give a measure of the degree of bond disorder introduced by the thermal motion and are thus related to the Anderson parameter W_t , see the right panel of Fig. 2.

Next, we address in more detail the influence of ZPF on the conductance. In Fig. 3 we show the averaged conductance for a fixed temperature with and without ZPF. We clearly see that ZPF do not have a sensitive influence on the behavior around the Fermi energy, i. e. on the lowest conductance plateau. However, the neglect of ZPF appreciably weakens the conductance suppression on the massive bands.

An important advantage of the FPA is the possibility to isolate the influence of *individual* vibrational modes on the electronic transport at a given temperature. In Fig. 4, we show the conductance $g_{\text{FP}}^{(n)}$ when *only* one eigenmode at the time is included in the transport calculation. In the figure, the x -axis labels both, the mode number n and its energy. Results are shown for two different electronic energies, indicated by arrows in Fig. 3. A general feature we can clearly see, is that electrons at the Fermi energy do not “see” the vibrational field, *i.e.* only few modes give a contribution to the conductance; moreover, the induced conductance change is much smaller than one percent. This illuminates farther our previous observation that near E_F the structure of the electronic spectrum is not appreciably changed when compared

with the zero temperature case. The other energy showed corresponds to a high-conductance plateau around 2.0 eV. On the latter, almost all vibrational modes are contributing. The reason is that enhanced backscattering related to channel mixing is more effective for massive bands and so the phase space available for scattering becomes larger. As shown in Fig. 4 (right panel), the neglection of ZPF reduces the contribution of the higher-lying modes, which are mainly C-C stretching bonds with different spatial patterns. The reason is that at the temperatures considered here (up to 500 K) the thermal occupation of these modes is basically negligible. As a result, the main contribution to the mode energy arises from the ZPF terms $\sim \hbar\omega/2$. Why the global conductance suppression *without* ZPF becomes much weaker, can be easily understood by looking at the typical length scales of the problem. The wave length of a tunneling electron is of the order of 0.5 nm , which is approximately of the same order as the length of the scattering region $l_{sc} \sim 0.7 \text{ nm}$. Low-frequency modes have wave lengths larger than l_{sc} , the opposite holding for high-energy modes. Hence, if the latter are inactive (no ZPF and negligible thermal factors), a propagating charge will mainly “see” long-wavelength distortions, which are less effective in scattering electrons.

Conclusions. – We have investigated signatures of structural distortions in the conductance spectrum of a metallic CNT. We found that the average effect of the lattice fluctuations may be qualitatively described by Anderson disorder. Our results point out that the linear bands crossing the degenerate Fermi points are not appreciably affected by structural fluctuations within the temperature range and length scales considered here. As a result, the theoretically expected conductance of $4 \times G_0$ is obtained. Massive electronic bands are however much more perturbed, their conductance being strongly reduced when comparing with the values of perfect CNTs.

The authors thanks P. Pavone for fruitful discussions. M. G. thanks the University of Regensburg for financial support. This work has been supported by the Volkswagen foundation.

REFERENCES

- [1] IIJIMA S., *Nature*, **354** (1991) 56; SAITO R., DRESSELHAUS G. and DRESSELHAUS M. S., *Physical Properties of Carbon Nanotubes*, Imperial College, London 1998; REICH S., THOMSEN C. and MAULTZSCH J., *Carbon nanotubes: Basic concepts and physical properties*, Wiley-VCH, Berlin 2004.
- [2] KANE C. L. and MELE E. J., *Phys. Rev. Lett.*, **78** (1997) 1932.
- [3] MCEUEN P. L. *et al.*, *Phys. Rev. Lett.*, **83** (1999) 5098.
- [4] SUZUURA H. and ANDO T., *Phys. Rev. B*, **65** (2002) 235412.
- [5] FIGGE M. T., MOSTOVLOY M. and KNOESTER J., *Phys. Rev. B*, **65** (2002) 125416; WOODS L. M., MAHAN G. D., *Phys. Rev. B*, **61** (2000) 10651.
- [6] EMBERLY E. G. and KIRCZENOW G., *Phys. Rev. B*, **61** (2000) 5740; FREDERIKSEN TH. *et al.*, *Phys. Rev. Lett.*, **93** (2004) 256601; PECCIA A. *et al.*, *Nano Lett.*, **4** (2004) 2109; CHEN Y.-C. *et al.*, *Nano Lett.*, **5** (2005) 621.
- [7] PECCIA A. *et al.*, *Phys. Rev. B*, **68** (2003) 235321.
- [8] ANANTRAM M. P. and GOVINDAN T. R., *Phys. Rev. B*, **58** (1998) 4882; HJORT M. and STAFSTRÖM S., *Phys. Rev. B*, **63** (2001) 113406; TRIOZON F. *et al.*, *Phys. Rev. B*, **69** (2004) 121410; WHITE C. T. and TODOROV T. N., *Nature*, **393** (1998) 240.
- [9] BABIC B. *et al.*, *Nanoletters*, **3** (2003) 1577; SAZONOVA V. *et al.*, *Nature*, **431** (2004) 284.
- [10] GHEORGHE M., GUTIERREZ R. and CUNIBERTI G., *unpublished*, (2004) .
- [11] FRAUENHEIM TH. *et al.*, *Phys. Stat. Sol. B*, **217** (2000) 41.
- [12] CUNIBERTI G., GROSSMANN F. and GUTIERREZ R., *Advances in Solid State Physics*, **42** (2002) 133.